IDENTIFICATION OF A CBF-β RUNX1 INHIBITOR WHICH BLOCKS HIV-1 INFECTION

by

Taylor Goad
A Thesis
Submitted to the
Graduate Faculty
of
George Mason University
in Partial Fulfillment of
The Requirements for the Degree
of
Master of Science
Biology

Committee:

_____	Dr. Yuntao Wu, Thesis Director
_____	Dr. Jia Guo, Committee Member
_____	Dr. Kylene Kehn-Hall, Committee Member
_____	Dr. James D. Willett, Director, School of Systems Biology
_____	Dr. Donna M. Fox, Associate Dean, Office of Student Affairs & Special Programs, College of Science
_____	Dr. Peggy Agouris, Dean, College of Science
Date: _____	Summer Semester 2015 George Mason University Fairfax, VA

Identification of a CBF-β RUNX1 Inhibitor Which Blocks HIV-1 Infection

A Thesis submitted in partial fulfillment of the requirements for the degree of Master of Science at George Mason University

by

Taylor Goad
Bachelor of Science
George Mason University, 2012

Director: Yuntao Wu, Professor
Department of Molecular and Microbiology

Summer Semester 2015
George Mason University
Fairfax, VA

ACKNOWLEDGEMENTS

I would like to thank my thesis advisor, Dr. Yuntao Wu, and my committee members, Dr. Jia Guo and Dr. Kylene Kehn-Hall for their guidance and support of this project. I would also like to thank Dr. Mark Spear for his mentorship and invaluable help throughout the course of this project. I also must thank all members of the Wu lab who have always been helpful during my time as a student. Finally, I would like to thank my parents, Bruce and Gail, for their unwavering support of me in all my pursuits. I could not have accomplished as much in my life without the encouragement they have continually provided.

TABLE OF CONTENTS

LIST OF FIGURES

ABSTRACT

IDENTIFICATION OF A CBF-B RUNX1 INHIBITOR WHICH BLOCKS HIV-1 INFECTION

Taylor Goad, M.S.

George Mason University, 2015

Thesis Director: Dr. Yuntao Wu

Human Immunodeficiency Virus (HIV) is a single-stranded RNA retrovirus and the causative agent of Acquired Immunodeficiency Syndrome (AIDS). Established antiretroviral therapy (ART) is mostly efficient in reducing viral load in patients, yet several circumstances may necessitate switching patients to new combination therapies. Drug incompatibility, serious side effects, and the emergence of drug resistance all illustrate the need for a wide selection of antivirals which can be used as second line drugs. After a preliminary anti-HIV drug screening, our lab has identified of a small molecule inhibitor of HIV-1 replication. This drug has been reported to block the association of two cellular transcription factors, CBF-β (core-binding factor subunit beta) and RUNX1. We demonstrate that this inhibitor blocks HIV infection by inhibiting viral transcription. Previous studies have also suggested that the viral protein Vif interacts with CBF-β, facilitating polyubiquitination and the degradation of the host restriction factor, APOBEC3G (A3G). Furthermore, the Vif-CBF-β binding interface may partially overlap with that of the CBF-β binding partner, RUNX1. Given that the identified drug is known to inhibit CBF-β - RUNX1 association, we are exploring the possibility that this

drug may also interfere with Vif-CBF-β interaction, facilitating the incorporation of A3G into budding viruses.

INTRODUCTION

Human Immunodeficiency Virus (HIV) is a single-stranded RNA retrovirus and the causative agent of Acquired Immunodeficiency Syndrome (AIDS). AIDS is characterized by the onset of a variety of opportunistic infections in otherwise healthy individuals alongside a concordant drop in the concentration of blood $CD4^+$ T cells to under 200 cells/μL. 35 million worldwide are estimated to be infected with HIV and there were an estimated 2.1 million new infections in 2013 [1].

New infections are concentrated (1.5 million of 2.1 million) in the World Health Organization (WHO) African region, which comprises most of the countries on the continent [1]. The virus significantly contributes to global mortality and morbidity figures, and as of 2012, AIDS-related illnesses were the 6th leading cause of death worldwide in terms of years of life lost [2]. Productivity and economic impacts of the pandemic in heavily afflicted countries are shaped by AIDS in dramatic ways and have been reviewed elsewhere [3]. Demographic structures have also shifted as a result of the virus: South Africa is estimated to have more than 2 million orphans from AIDS related deaths alone [4].

Despite a strong international effort to mitigate viral spread and a consistent drop in the global rates of new HIV infections for over 10 years, the epidemic persists, warranting continued international action[1]. Increases in new infections have even been

reported in some world regions in the midst of the strongest international effort yet to combat the virus [1]. The pandemic is also becoming a greater concern due to high rates of HIV and tuberculosis (TB) co-infection. HIV-infected individuals are 29 times as likely to develop TB than uninfected residents of the same country [5]. These concerns are further compounded by the difficulties which arise when responding to disease in impoverished regions such as access to and affordability of therapeutic agents. These factors, in conjunction with the chronic nature of the disease, suggest the ongoing struggle to control the spread of the virus will require concerted international effort for quite some time.

HIV life cycle

HIV-1 infects human CD4 T cells, macrophages, dendritic cells (DC), and natural killer (NK) cells [6,7]. The primary targets *in vivo* are CD4 T cells and macrophages, with $CD4^+$ effector memory cells being significantly depleted upon disease progression [8]. HIV-1 enters target cells by receptor-mediated fusion with the host cell membrane. The HIV surface glycoprotein, GP120, binds CD4 receptors on target cells. Binding induces a conformational change in GP120 which promotes interaction with the cellular chemokine receptors CXCR4 or CCR5. Conformational changes in gp120 expose the fusion domain of the viral envelope protein, gp41. In a manner similar to that of influenza fusion, gp41 mediates the merger of the viral envelope with the host cell membrane.

Upon entering the target cell, HIV-1 interacts with the cortical actin to facilitate reverse transcription, uncoating, and nuclear import [9]. Upon reaching the nucleus, viral

DNA integrates into the host genome, typically at sites of active chromatin. Short, fully-spliced viral transcripts are produced early in the viral life cycle, and their products act to promote translation of later partially-spliced and unspliced transcripts. HIV Gag structural proteins polymerize at sites on the plasma membrane in lipid raft domains where conformational changes within Gag couple virion assembly, packaging of the viral genome, and budding.

Disease progression

Resting T cells represent the most abundant target of HIV-1 *in vivo*, as the majority of T cells in the body are in a resting state [10]. HIV is unique among other viruses in the fact that it can infect these non-dividing cells. Despite reports of several post-entry blocks to the viral life cycle, production of HIV-1 has been achieved from resting CD4 T cells after *in vitro* infection and subsequent activation [10]. *In vivo*, this situation is thought to be slightly different as local cytokine environments may render resting cells slightly more permissive for viral replication than the stricter, *in vivo* scenarios [10]. Once activated, CD4 T cells are highly permissive for HIV replication and support high viral yield.

HIV infection results in a rapid depletion of mucosa-associated T cells within weeks of initial infection [8,11]. These areas are rich in effector memory T cells (TEM), and this subset undergoes a dramatic depletion during the acute phase of infection [8]. Despite this depletion, immune functions are maintained throughout much of the chronic phase of infection, and the host maintains the ability to fight opportunistic infections for up to several years in some cases [12]. After the initial depletion of $CD4^+$ T cells, the peripheral

blood $CD4^+$ T cell count of HIV patients starts to recover, evidence of the preserved regenerative potential of uninfected naive and central memory $CD4^+$ T cells (TCM). Yet despite this potential for regeneration, $CD4^+$ counts in HIV patients slowly start to decline again in the chronic phase of infection, usually concomitant with the onset of opportunistic infections.

Progression to AIDS is thought to occur as the result of depleted T cell numbers due to a state of chronic immune activation, yet the process is incompletely understood. Studies in non-human primates illustrate the intricacies of immune homeostasis in disease progression. Simian immunodeficiency virus (SIV) infection in sooty mangabeys does not result in AIDS, but does cause disease in rhesus macaques. In rhesus macaques, TCM proliferation is negatively associated with disease progression, whereas TCM proliferation is positively associated with disease progression in sooty mangabeys [13]. Similarly, in humans, T cell activation has been shown to correlate positively with reduced CD4 T cell gains upon the start of ART as well as the onset of AIDS [14]. The phenomenon of suboptimal immune reconstitution in humans is not fully understood, but of note is the observation that antiretroviral therapy has been shown to result in decreased T cell activation [15]. Despite the lack of a complete understanding of this phenomenon, early antiretroviral therapy during primary infection has also been shown to help preserve the numbers and responses of HIV-directed $CD8^+$ T cells as well as preserve the presence of an HIV-directed $CD4^+$ T cell response[16]. Conversely, the absence of early intervention correlates with poor HIV-directed $CD8^+$ and $CD4^+$ T cell responses [16].

Antiretroviral therapy

A number of features of the life cycle of HIV make the virus especially hard to treat. One of the most important is the capacity of HIV to infect long-lived resting CD4 T cells. The estimated mean half-life of CD4 T cells is 44 months, with a complete decay of an infected subset of cells taking up to 60 years [17]. As these cells remain in a resting state, there is no active viral replication and immune recognition of these latently infected cells rarely occurs. This population of inactive, latently infected cells makes complete eradication of the virus from patients impossible to achieve with current ART therapy.

Despite these barriers to treatment, effective therapeutics have been developed which are mostly successful in suppressing viral load in patients. The advent of antiretroviral therapy for HIV-1 treatment has drastically extended the lives of HIV-1 infected individuals. Adherence to a combination therapy can extend the life expectancy of HIV-1 patients to that of uninfected individuals with other chronic illness or unhealthy lifestyles [18]. Longitudinal follow ups on US patients estimate that from 1994 to 1998, the rate of opportunistic illness in HIV-infected patients declined from 23.7 events per 100 person-years to 14 events per 100 person-years [19]. The rate of AIDS related deaths in the US also declined 23% from 1995 to 1996 [20]. This decline coincided with, and is largely attributed to an increase in the frequency of prescription of combination therapy for HIV patients in 1996 [20].

Antiretrovirals have also proved to be effective in the areas of the world most affected by HIV/AIDS. UNAIDS estimates that antiretrovirals have averted 5.5 million deaths in low- and middle-income countries between 1995 and 2012 [21]. A case study is the rural KwaZulu-Natal province in South Africa. Between 2000 and 2003, adult life

expectancy declined from 55.4 to 51.3 years for women and from 49.0 to 46.9 years for men [22]. ART then became available through the public sector health system to this region in 2004, and is thought to be responsible for a subsequent gain of 11.3 years in average adult life expectancy between 2003 and 2011 [22].

The success of combination therapy is partly due to the availability of different classes of antiretroviral drugs. The use of any drug to treat HIV selects for the development of drug resistance within the patient's body. One advantage of combination therapy comes from the decrease in the likelihood of simultaneous drug resistance mutations emerging in the same round of viral replication. US Food and Drug Administration (FDA) approved HIV antiretrovirals include compounds that inhibit several viral processes such as engagement of cellular receptors, membrane fusion, reverse transcription, and polyprotein cleavage. The US Department of Health and Human Services (HSS) now advises the use of an integrase, protease, or non-nucleoside reverse transcriptase inhibitor usually alongside 2 nucleoside reverse transcriptase inhibitors for the treatment of HIV-1 patients [23]. These antiretrovirals are increasingly able to reach high risk populations in low and middle income countries, and as of 2012, 7.5 million people in the WHO African region [24]. Mother to child transmission of HIV has also been greatly reduced as a result of the ever widening accessibility of antiretrovirals. Mother to child transmissions of HIV dropped 58% between 2002 and 2013 [25].

Despite the availability of effective drugs for HIV-1 treatment, there are several complications which may arise during treatment that necessitate switching a patient to a

different combination therapy. These include side effects from a given antiviral, poor drug absorption, drug-drug interactions, drug-food interactions, regimen adherence, and emergence of drug resistance [26]. The World Health Organization (WHO) estimates that 10% - 17% of antiretroviral (ARV) - naive HIV-1 patients in high-income regions such as Europe, the US, Japan, and Australia are infected with at least one viral strain with resistance to an antiviral drug [27]. Similarly, a study of HIV-1 patients in 15 European countries estimated that in patients undergoing virologic failure, 80.7% had a viral mutation conferring drug resistance [27]. The reduction in transmission rates and overall disease burden that have been achieved by the increasing availability of antiretrovirals in both low and high-income countries represents a very promising trend for the future of the HIV/AIDS pandemic, yet care must be taken to effectively manage the use of HIV drugs in order to control the spread of drug resistance. It is therefore prudent for healthcare providers to have a wide selection of antivirals that can be used as second line drugs in the case of virologic failure, and to manage the prescription and use of these carefully.

HIV transcription

Transcription of viral proteins is driven by the HIV long terminal repeat (LTR) region which acts as a promoter. The LTR contains enhancer and promoter elements for viral genes, and transcription of these is driven primarily by the cellular transcription factors NF-KB and Sp1 [28]. The viral LTR can additionally recruit both activating and repressing cellular factors, and the identities of these effect the final level of transcription from the promoter [29]. The newly integrated viral promoter efficiently initiates

transcription of viral genes, but the associated transcriptional complex lacks processivity and its major products are short and truncated transcripts [30]. Virally encoded Tat protein counteracts this normal state by transactivating transcription by binding to a viral transcriptional activation region (TAR) in the first 59 nucleotides downstream from the viral transcription start site [28]. This sequence element forms a stem-loop construct in nascent mRNA transcripts which acts as a docking site to coordinate the formation of an activation complex. Tat coordinates the recruitment of transcription factors to the TAR, promoting hyperphosphorylation of nearby RNA polymerase II, increasing its processivity [31].

CBF-β

The cellular transcription factor, Core-binding factor subunit beta (CBF-β), forms a transcriptional complex with Runt-related transcription factor (RUNX) family transcription factors to drive the expression of genes related to cellular differentiation and hematopoiesis [32]. CBF-β does not bind DNA elements directly, instead it stabilizes and regulates the folding and DNA binding ability of the RUNX member to which it is bound [32]. RUNX1 is primarily localized in the nucleus, while CBF- β is found distributed throughout both the nucleus and cytoplasm [33].

Recent literature has reported that the HIV-1 accessory protein, Viral infectivity factor (Vif), hijacks CBF-β in order to polyubiquitinate and degrade the host restriction factor, apolipoprotein B mRNA editing enzyme, catalytic polypeptide-like 3G (A3G) [34]. A3G is thought to function within the cell to regulate cell cycle as well as control parasitic DNA elements such as Alu and LINE-1 retrotransposons [35,36]. A3G bears

significant relevance to HIV in its ability to restrict viral replication. In the absence of HIV Vif, A3G becomes incorporated into budding viruses, and impedes viral replication during the subsequent round of reverse transcription via cytidine deamination of viral cDNA and steric blocking of the viral reverse transcription complex [37]. Vif can degrade A3G, thus preventing this particular method of viral restriction within infected cells. Vif counteracts A3G by targeting it for polyubiquitination and subsequent degradation via the proteasome [38]. Vif-mediated A3G polyubiquitination occurs via the assembly of a cytoplasmic multiprotein complex consisting of Vif, CBF-β, A3G, CUL5, RBX2, and the adaptors elongin B and elongin C [38]. This interaction occurs in normal infection of lymphocytes, and thus is not likely to play a major role in restricting viral spread *in vivo*.

A recent study suggests that the binding of CBF-β to Vif is mutually exclusive with normal binding of CBF-β to RUNX transcription factors, as a CBF-β/Vif/ELOBC complex fails to bind RUNX even when RUNX is in molar excess of 16 fold [38]. Kim *et al.* suggest this may be due to overlapping RUNX and Vif binding domains on CBF-β. Despite this, conflicting data exist regarding the ability to co-immunopurify Vif with RUNX, which if possible, would indicate CBF-β can bind both these proteins simultaneously. Understanding the nature of the binding between these three proteins is important for the development of drugs that interfere with Vif-mediated A3G degradation. Drugs that interfere with CBF-β binding sites could block the formation of the polyubiquitin complex and prevent A3G degradation, facilitating its incorporation into budding viruses and restricting viral spread. Our lab has obtained a compound which we believe may act in this manner as well as inhibiting viral transcription.

TIME OF ADDITION STUDY

Background

The drug NSC 156594 was obtained as part of a diversity drug discovery set through the National Cancer Institute's (NCI) Developmental Therapeutics Program (DTP). A large scale screening of this set in our lab identified several drug candidates (unpublished data). The impact of this drug on HIV replication is also supported by a National Cancer Institute AIDS Antiviral Assay screening. NSC 156594 has been shown to inhibit HIV-1 mediated cytotoxicity as determined by formazan-based cell viability assay [39]. The National Cancer Institute AIDS Antiviral Assay works by the addition of tetrazolium reagent to *in vitro* cell culture that is metabolized by viable cells into a formazan product that can be colorimetrically detected [40]. As such, this assay quantifies the degree of cellular metabolic activity, and not viral replication directly. To gain a better idea of the effect of this drug on the HIV life cycle, we performed a time of addition drug study, whereby drug is added to the cell culture at various time points before and after infection. The time point at which inhibition is observed will therefore suggest a time frame for the process of the viral life cycle upon which the drug may be acting.

Materials and Methods

Indicator cell line

Clone-X indicator cells were used for preliminary drug concentration and time of addition studies. Briefly, Clone-X cells are a derivative of the previously described Rev-CEM cell line [41]. These are a CEM-SS based cell line which expresses *luciferase* and *gfp*

transcripts containing a Rev Response Element (RRE). This exploits the natural shuttling of RRE-containing viral transcripts out of the nucleus in the presence of the HIV-1 protein, Rev. In the absence of infection, no viral Rev protein is present to export reporter transcripts to the cytoplasm, and RRE-containing transcripts are subsequently degraded after transcription. Conversely, upon HIV-1 infection, RRE-containing reporter transcripts are exported to the cytoplasm where they are translated to yield Firefly Luciferase and GFP. Cells were maintained at a concentration under $1e^6$ cells/mL and cultured in RPMI (Life Technologies) +10% fetal bovine serum (Life Technologies) at 37°C and 5% CO_2.

Infection

$2e^5$ Clone-X cells were aliquoted in 5 mL tubes in a volume of 100µL RPMI +10% FBS. Working stock of NSC 156594 was made by diluting the drug in dimethyl sulfoxide (DMSO) to a concentration of 5 mM. Drug was added to a final concentration of 50 µM at the following time points relative to time of infection: 12 hours pre, 6 hours pre, 1 hour pre, at time of infection, 2 hours post, 6 hours post, and 12 hours post. Pre-treatment and post-treatment controls of DMSO were added either 12 hours before infection or 12 hours after infection. 200µL (approximately 200-250ng) of wild-type NL3-4 was added to the cell culture and drug or DMSO was added back to maintain concentration. After infection, cell cultures were incubated at 37°C and 5% CO_2. Cultures were then washed twice in serum free RPMI, and resuspended in 1 mL of RPMI +10% FBS. For spinoculated infections, cell cultures were infected as described, but placed immediately into a centrifuge and spun at 600 x g for the 2 hour infection period. Washes were then performed as described above.

Luciferase assay

Samples were analyzed according to Promega's Luciferase Assay. Briefly, 200µL of cell culture was harvested and centrifuged at 12,000rpm for 5 minutes. Supernatant was aspirated off the cell pellet, and 120µL of 1x reporter lysis buffer (Promega) was added to lyse and resuspend the cell pellet. 100µL of lysate was then loaded onto a 96-well plate for quantification in a GloMax-Multi (Promega).

Flow Cytometry

Propidium iodide was added to cell cultures to mark dead cells and then analyzed on BD FACSCalibur flow cytometer. Forward scatter and side scatter channels were used to differentiate between the healthy population of cells and those that were dying. A primary gate was applied to the population of healthy cells. A secondary gate was then created from the negative control and applied to the experimental samples to record events representing HIV-1 infected, GFP-producing cells.

Results

A Rev-dependent reporter cell line (Clone-X) was used to quantify the degree of NSC156594-mediated inhibition of HIV-1 replication. Preliminary data from our lab showed 78% inhibition of HIV-1 replication at a drug concentration of 50 µM as determined by flow cytometry (data not shown). A time of addition study was then performed to gain a rough idea of the stage(s) of the viral life cycle upon which the drug was acting. Drug was added to Clone-X culture at 12 hours, 6 hours, and 1 hour before infection, as well as at time of infection, 2 hours, 6 hours, and 12 hours after infection. Inhibition was most obvious when drug was added before infection with maximal inhibition (58%) observed at the 6 hour pre-treatment time point (Figure 1). Later time

points also showed inhibition, albeit less dramatic than pre-treatment time points. Post infection time points were limited to 35% inhibition at 2 hours post-treatment. Analysis of the infections via luminometry supports the findings via flow cytometry. The highest inhibition is seen in the 6 hour pre-treatment time point, with a lessening impact at progressively later time points (Figure 2). These data suggest that the drug may interfere with one of the early steps in the viral life cycle. Plausible targets may be entry, reverse transcription, integration, or early transcription. Conversely, late stages of the viral life cycle are unlikely to be the point where this drug is acting, as viral inhibition generally tended to be less at these times of addition.

Due to the low infection rates of the first time of addition study, the experiment was repeated using spinoculation, a process whereby cell cultures are centrifuged during a 2 hour infection. This process has previously been shown to increase actin dynamics, facilitating increased viral infection [42]. Spinoculation was used in the hopes of amplifying the degree of viral infection, thus accentuating any inhibition profiles that may be present. When analyzed via flow cytometry, slightly greater maximal inhibition was observed when the samples were spinoculated during infection compared to the non-spinoculated infection. 66% inhibition was observed at the 1 hour pre-treatment FC time point (Figure 3). Similarly, post-treatment time points also showed greater inhibition than the original time of addition experiment with 53% inhibition at the 6 hour post infection FC time point.

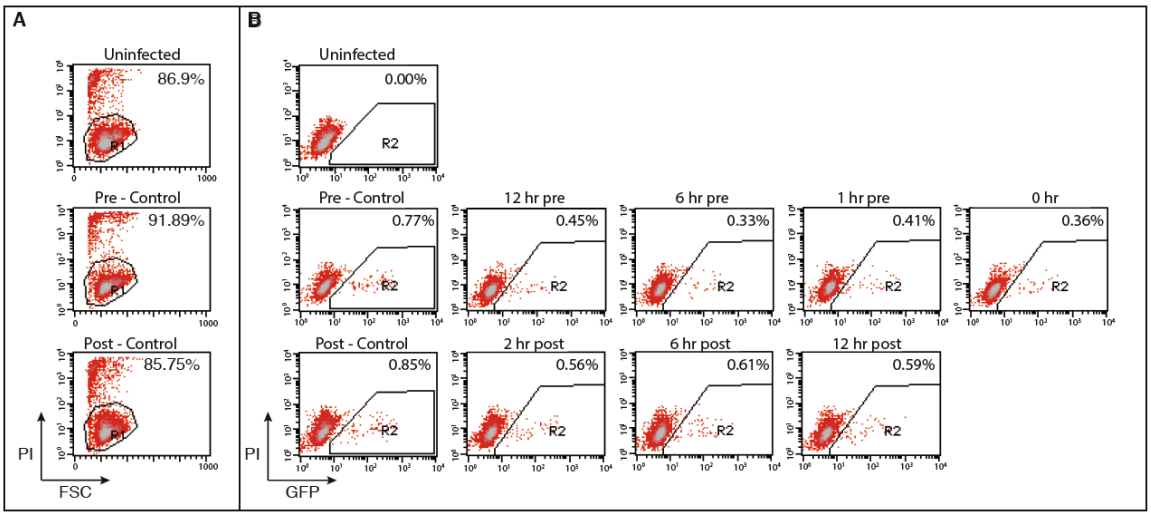

Figure 1. NSC 156594 inhibits viral replication in CloneX cells.

CloneX cells were infected for 2 hours and treated with 50 µM NSC 156594 at the indicated time points relative to the time of infection. 72 hours after infection, cell culture aliquots were stained with propidium iodide and assayed via flow cytometry to assess cell viability (propidium iodide) and HIV infection (GFP). *(A)* Primary gates were applied to the negative control, pre-control and post-control to identify the healthy cells. (*B)* A secondary gate was then created and applied to the population of healthy cells to identify the HIV-infected subpopulation. The gate in the bottom right corner of each plot contains viable cells with high GFP intensity, indicative of HIV-infected cells. Percentages given indicate percent of the gate 1 (healthy) population which also appear in the secondary gate (HIV-infected).

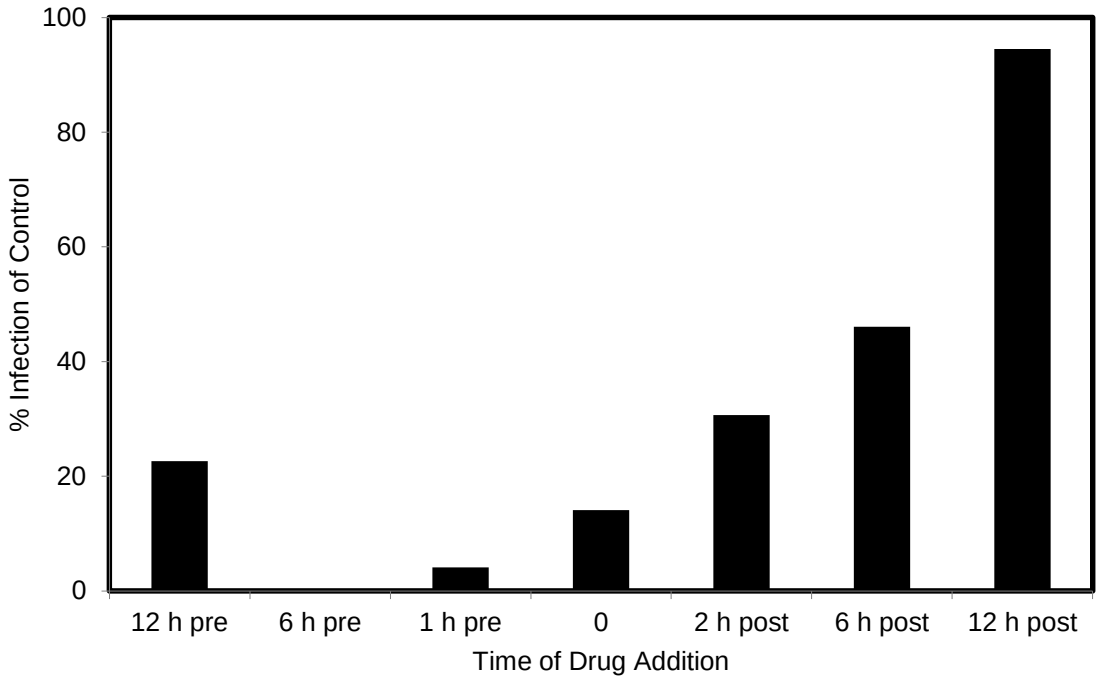

Figure 2. NSC 156594 inhibits viral replication in CloneX cells.

CloneX cells were infected for 2 hours and treated with 50 µM NSC 156594 at the indicated time points relative to the time of infection. 200µL aliquots of cell culture were pelleted and lysed in 120µL of lysis buffer. 100 µL of lysate was loaded onto a 96 well plate for quantification. Results shown are lysates taken from cell culture 72 hours after infection.

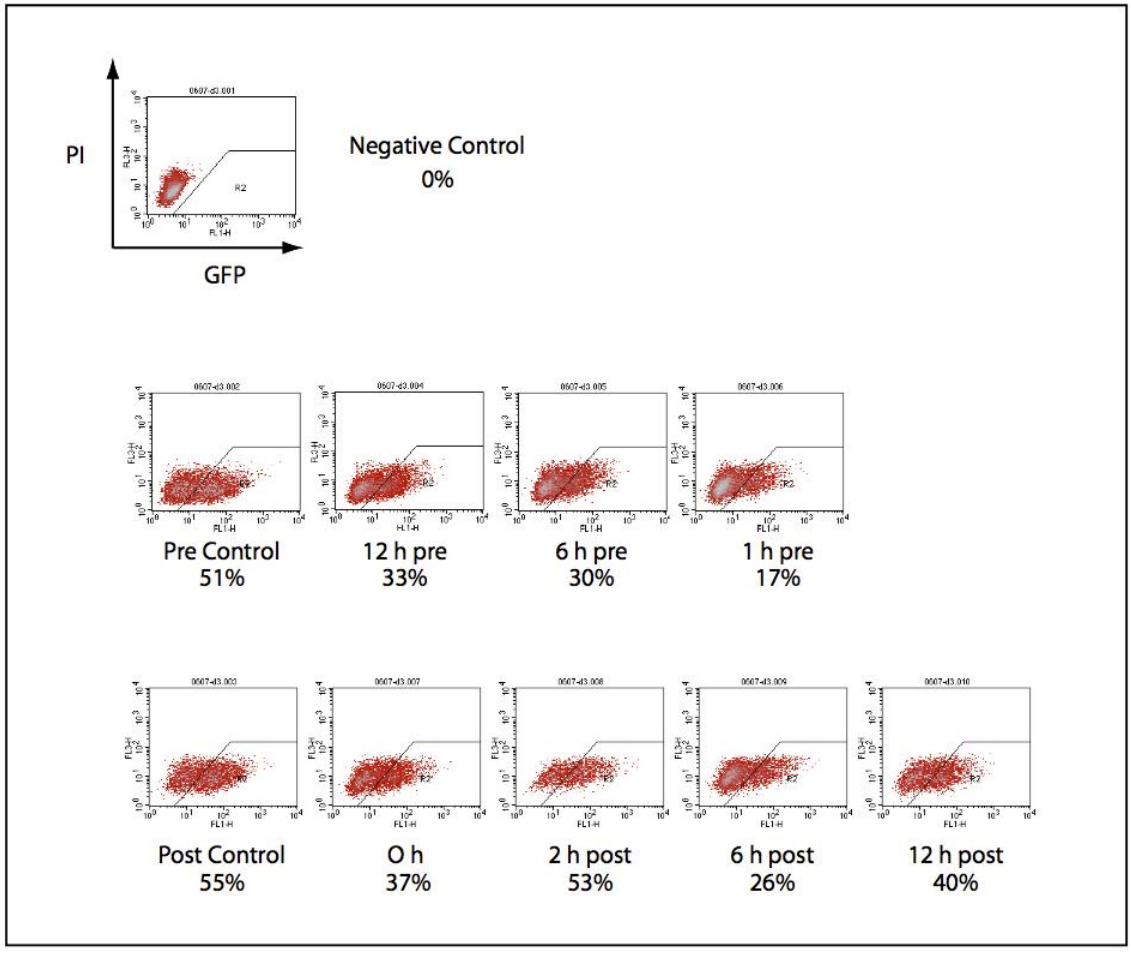

Figure 3. NSC 156594 inhibits HIV-1 maximally at pre-treatment time points

Clone-X cells were infected for 2 hours with spinoculation at 600 x g. 72 hours after infection, cell culture aliquots were stained with propidium iodide and assayed via flow cytometry to assess cell viability (propidium iodide) and HIV infection (GFP). The gate in the bottom right corner of each plot contains viable cells with high GFP intensity, indicative of HIV-infected cells. Percentages given are the percent-infected of the total population of viable cells.

A noteworthy difference from the previous assay was seen in the luminometry-derived data (Figure 4). When analyzed via this method, 6 hour and 12 hour post infection time points showed high levels of inhibition (66 and 67% inhibition, respectively). Variation was also seen between spinoculated and non-spinoculated sample data from the same quantification method. Some degree of variation between these is expected, as the metabolic state of actin dynamics has been altered and other tangential pathways are also likely to have been altered. It is also worth considering the possibility that multiple modes of action may obfuscate the actual nature of the inhibition, and result in inconsistent inhibition profiles. As the point of this assay was to gain an estimate of the time frame of inhibition, further experiments were not performed to stabilize the data. Rather than repeat this study, we decided to assay DNA and RNA synthesis in drug treated samples.

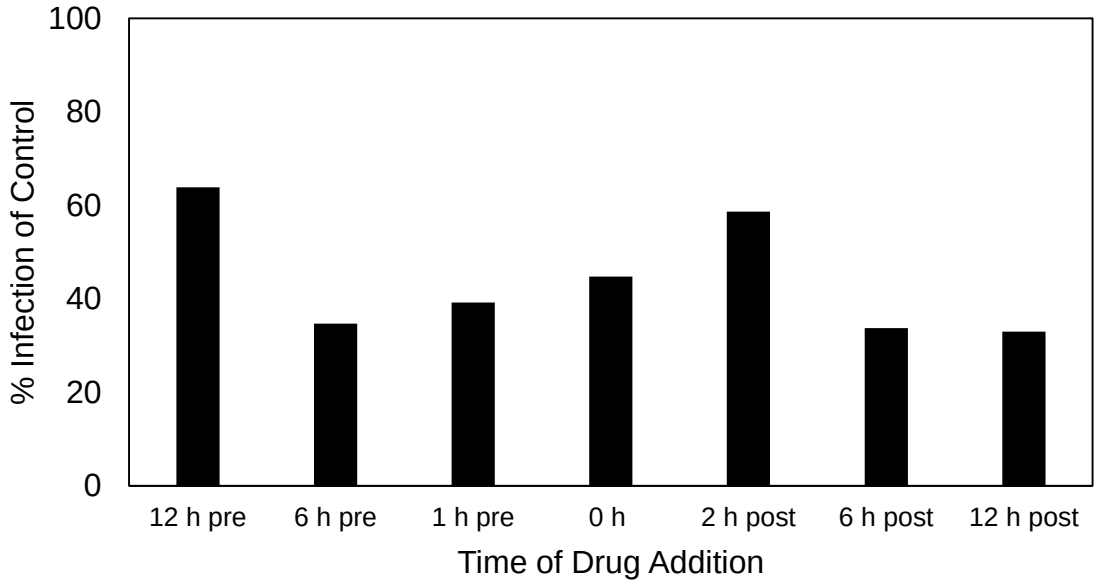

Figure 4. NSC 156594 inhibits HIV-1 at both early and late time

Clone-X cells were infected for 2 hours with spinoculation at 600 x g. Cells were analyzed 48 hours after infection. 200µL aliquots of cell culture were pelleted and lysed in 120µL of lysis buffer. 100 µL of lysate was loaded onto a 96 well plate for quantification. Results shown are a representative result of 1 of 3 reads via luminometry.

DNA AND RNA SYNTHESIS

Materials and Methods

Cell culture

CEM-SS cells were cultured in RPMI (Life Technologies) supplemented with 10% fetal bovine serum (Life Technologies) plus penicillin (100 U/mL) and streptomycin (100 µg/mL) (Life Technologies) at 37°C and 5% CO_2.

Infection and sample collection

$7.5e^6$ CEM-SS cells each were aliquoted into 2, 12 mL round bottom tubes at a concentration of $1.5x10^6$ cells/mL. Cells were pre-treated by adding 50µL of 100X drug working stock (NSC 156594 diluted in DMSO to 5mM) or undiluted DMSO to the cell cultures 1 hour before infection. A 0 hour sample of cell culture was collected at this time. Cells were infected by pelleting the cell culture, discarding supernatant and adding 1mL (approximately 200-250ng) of single cycle HIV-$1_{NL4\text{-}3\Delta\Psi}$ (Env) to each tube. 10µL of 5mM drug or DMSO was added to maintain concentration. Infected cell cultures were then incubated for 2 hours at 37°C and 5% CO_2. Cells were washed twice with 6mL of serum free RPMI (Life Technologies) by pelleting at 300 x g for 5 min at room temperature, discarding supernatant and resuspending in 4mL RPMI+10%FBS. 40µL of 100X drug or DMSO was then added to maintain concentrations. Samples were collected at 2 hours, 6 hours, 12 hours, 24 hours, and 48 hours relative to the time of infection. Samples were collected by removing 1mL of the cell culture, pelleting cells, vacuuming out the supernatant, adding 400µL of RNA lysis buffer to the cell pellet. At 12 hour and

24 hour time points, 500µL of fresh RPMI+10%FBS was added back to each tube along with 5µL of 100X drug or DMSO.

DNA and RNA isolation

Total DNA extracted using the Wizard SV Genomic Purification System according the manufacturer's protocol (Promega). RNA was extracted using the SV Total RNA Isolation System according to the manufacturer's protocol (Promega).

DNA and RNA isolation

Total DNA was extracted using the Wizard SV Genomic Purification System according the manufacturer's protocol (Promega). RNA was extracted using the SV Total RNA Isolation System according to the manufacturer's protocol (Promega).

Quantitative PCR and RT-PCR

Total Viral DNA was quantified by quantitative PCR using oligonucleotide primers (Integrated DNA Technologies): HIV-Env-5F (5'-GCGGGAGAATGATAATGGAGAAAGG-3'), HIV-Env-3R (5'-GGCCTGTGTAATGACTGAGGTGTT-3'). To detect total viral DNA, an oligonucleotide probe was used which contains a 5' located 6-FAM fluorophore and a 3' located Black Hole Quencher (Integrated DNA Technologies): Env-Probe (5'-56FAMTCAGCACAAGCATAAGAGATAAGGTGCAGA-3BHQ-3'). Viral DNA, pNL4-3, mixed with genomic DNA from CEM-SS was used as a standard set for this assay with copy numbers of 1 to 10^6.

2-LTR circles were also quantified via qPCR, using oligonucleotide primers (Integrated DNA Technologies): MH536 (5'-TCCACAGATCAAGGATATCTTGTC-3'), MH535 (5'-AACTAGGGAACCCACTGCTTAAG-3'). The probe for 2-LTR circles

also utilized a 5'6-FAM fluorophore and a 3'Black Hole Quencher (Integrated DNA Technologies): MH603 (5'-56FAMACACTACTTGAAGCACTCAAGGCAAGCTTT-36TAM-3'). The standard for 2-LTR circle synthesis was a cloned plasmid which contains a full 2-LTR region. This plasmid, pLTR-2C, was made by amplifying the DNA of infected cells with the primers: 5'-TGGGTTTTCCAGTCACACCTCAG-3' and 5'-GATTAACTGCGAATCGTTCTAGC- 3'.

cDNA *nef* transcripts were quantified via qPCR using the primers: 5′ Nef (5′-GGCGGCGACTGGAAGAA-3′), 3′ Rev (5′-AGGTGGGTTGCTTTGATAGAGAAG-3′), and the probe Nef/Rev (5′-FAM-CGGAGACAGCGACGAAGAGCTCATC-TAMRA-3′).

cDNA synthesis

Extracted RNA was used for cDNA synthesis in a reaction containing 10X complete PCR buffer, 2.5mM dNTPs, random decamer primers, an RNAse Inhibitor (Life Technologies), and M-MLV Reverse Transcriptase (Life Technologies). The cDNA synthesis was assembled and incubated at 42°C for 1 hour, followed by a heat inactivation at 92°C for 10 minutes.

Results

A quantitative PCR (qPCR) for total viral cDNA was performed to determine any effect of NSC 156594 on viral cDNA synthesis. In activated T cells, reverse transcription occurs shortly after entry, with the subsequent cDNA transcripts building up between 4 to 6 hours post infection [43]. The probes used in this assay are complementary to viral cDNA, and provide a measure of the degree of reverse transcription.

Single cycle HIV-$1_{NL4\text{-}3\Delta\Psi}$ (Env) virus is incapable of undergoing a second round of replication after the initial infection of the target cell. The use of this virus limits the application of any results to a single round of replication, but eliminates any potential distortions from the additive results of multiple rounds of viral replication. While this is a standard protocol used in our lab to analyze drug effects on the viral life cycle, there is additional relevance to the topic of study in this investigation. Because we suspect A3G degradation, and thus function, may be effected by the drug, there is the possibility that multiple rounds of replication with drug treatment will allow this effect to be observed. This could possibly obscure any effects which the drug may exert on other stages of infection. The previously conducted time of addition study did not use single cycle virus, and difficulties arise when drawing conclusions about the nature of the inhibition from these previous data.

Minor inhibition (15%) was observed in 6 hours and 12 hours post infection time points, but were not sufficient to explain the significant inhibition observed in the previous FC results (Figure 5). Indeed, this inhibition was not reproducible across multiple repetitions of the experiment (data not shown). At 24 hour and 48 hour post-infection time points, there was some enhancement of DNA synthesis in the drug-treated sample relative to the DMSO-treated control, but again these data were not sufficient to explain the previously observed inhibition of replication. The lack of any clear difference in total viral DNA synthesis suggests that NSC 156594 does not impact this step of the viral life cycle. Furthermore, it is unlikely that it effects any earlier steps in the life cycle.

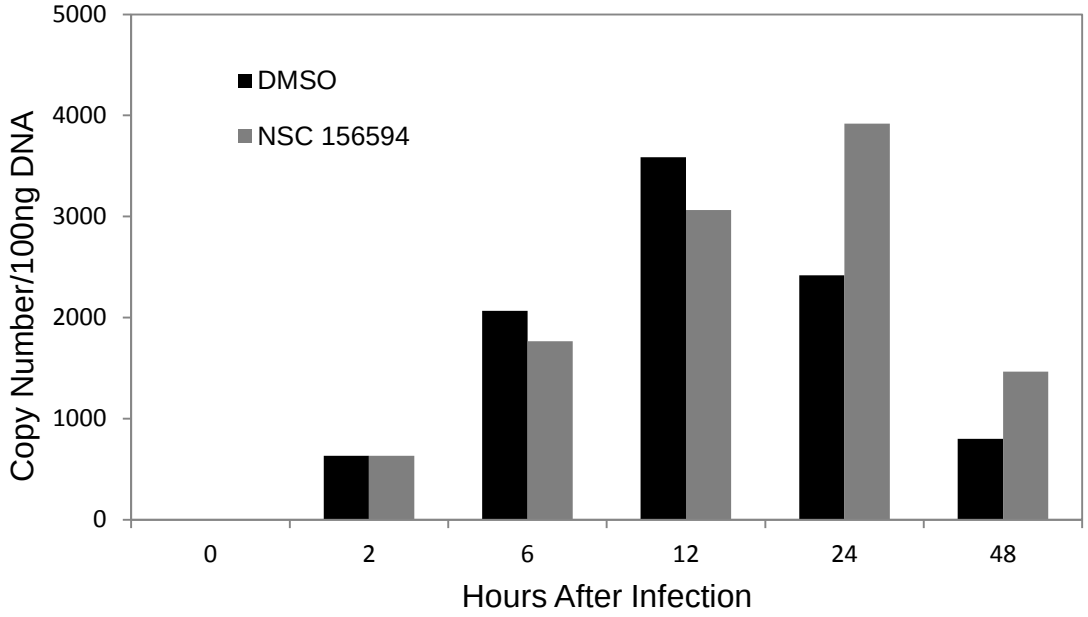

Figure 5. NSC 156594 does not inhibit total DNA synthesis.

$7.5e^6$ CEM-SS cells were infected with single cycle, HIV-$1_{NL4\text{-}3\Delta\Psi}$ (Env) virus for 2 hours. Cell cultures were washed, and samples were collected at the indicated time points for subsequent DNA extraction. Extracted DNA was analyzed via qPCR. Data shown are a representative result of the total DNA assay.

If a step such as entry was impacted by this drug, the difference between the drug treated group and the DMSO control should have been picked up in this assay. Therefore, it was concluded that viral engagement of cellular receptors CD4 and CXCR4, fusion, uncoating, and reverse transcription are not targets of this drug**.**

Next, the presence of 2-LTR circles was quantified via qPCR. 2-LTR circles are viral cDNA genomes which occur as a natural byproduct when host DNA repair machinery acts on linear, viral DNA through the non-homologous end joining pathway [44]. These therefore only form in the nucleus, and can be interpreted as a measure of nuclear localization of viral cDNA [45]. Figure 6 shows the average of 3 independent assays for 2-LTR circles. Large variances in the data set were observable, likely due to low number of 2-LTR circles found in infected cells as well as observer influence. Despite these variances, there was no apparent difference in 2-LTR circles between drug- and DMSO-treated samples. It is therefore likely that NSC 156594 inhibits neither nuclear migration nor import of the pre-integration complex (PIC).

We then decided to determine any effects of the drug on early viral transcription. *Nef* cDNAs were synthesized via RT-PCR, which were then used for qPCR. Low *nef* transcript synthesis was observed in both drug-treated and control samples at 2 hours post infection through 12 hours post infection (data not shown). *Nef* transcript synthesis remained at either undetectable levels or maximally 2.4 copies per 12.5 ng RNA during these time points. At 24 hours post infection, the drug-treated sample yielded only 29% of the number of *nef* transcripts as the DMSO-treated control, corresponding to a 70%

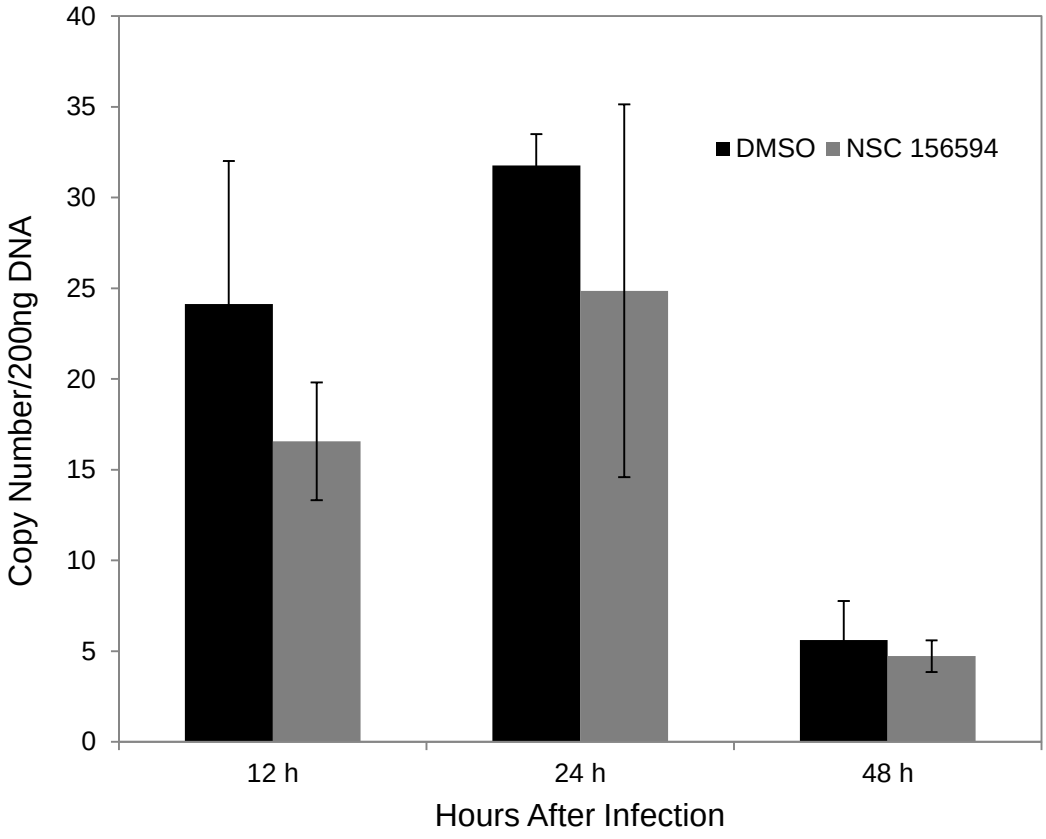

Figure 6. NSC 156594 does not inhibit 2-LTR circle synthesis.

$7.5e^6$ CEM-SS cells were infected with single cycle, HIV-$1_{NL4\text{-}3\Delta\Psi}$ (Env), virus for 2 hours. Cell cultures were washed, and samples were collected at the indicated time points for subsequent DNA extraction. Extracted DNA was analyzed via qPCR. Data shown indicate the average of 3 separate experiments quantifying 2-LTR circles.

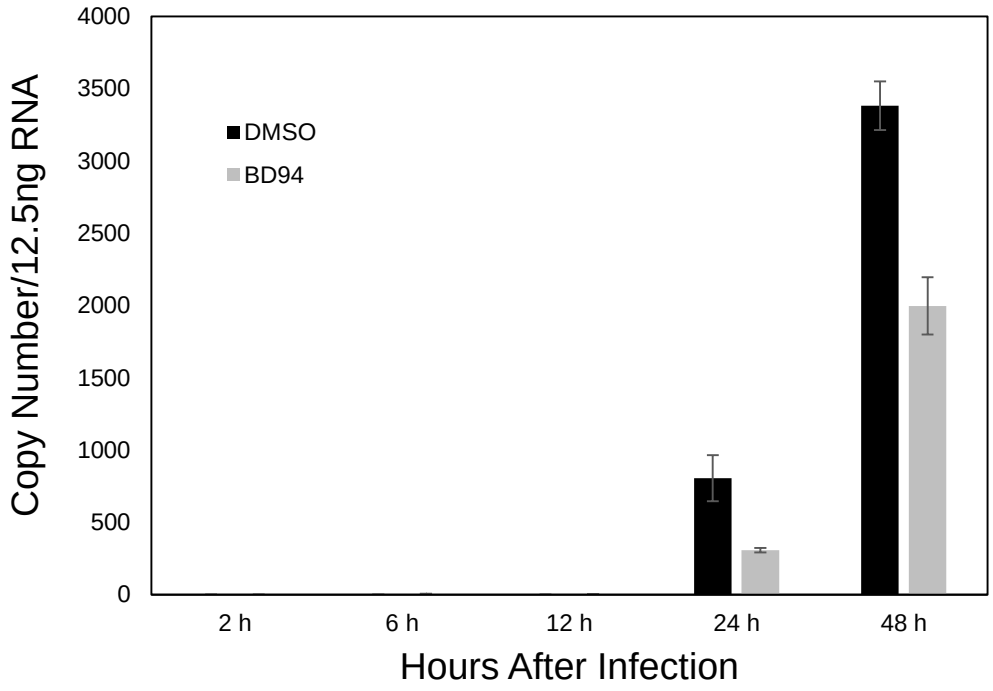

Figure 7. NSC 156594 inhibits *nef* transcription.

$7.5e^6$ CEM-SS cells were infected with single cycle, HIV-$1_{NL4\text{-}3\Delta\Psi}$ (Env), virus for 2 hours. Cell cultures were washed, and samples were collected and lysed at the indicated time points for subsequent RNA extraction. Extracted RNA was analyzed via qPCR after cDNA synthesis. Data shown indicates the average of two duplicate wells run for each sample.

reduction in *nef* transcript synthesis. Similar inhibition, though not as dramatic, was observed in the 48 hours post infection sample. At this time point, drug-treated samples showed 50% less *nef* transcript synthesis than the control.

This assay was repeated with the same set of cDNA samples to confirm the observed results with another qPCR. Upon repetition, the same pattern of *nef* transcript inhibition was observable (Figure 7). Again, all *nef* transcripts were low at early time points (2 hours post infection through 12 hours post infection), and a difference in copy number became apparent in 24 and 48 hour post infection time points. Drug-treated samples at 24 hour time point contained 61% fewer *nef* transcripts than the control. At 48 hours post infection, the drug-treated samples contained 41% fewer transcripts than the control.

These data indicate that NSC 156594 may interfere with proviral transcription. Because we did not test integration directly, we cannot rule out an impact of the drug on integration. The lack of a difference in 2-LTR synthesis may suggest that integration is not targeted by this drug. cDNA that fails to integrate into the cellular genome forms 2-LTR circles [46]. Any impact on integration should therefore be detected in the number of 2-LTR circles. Still, it may be useful to perform an Alu-LTR PCR assay for proviral integration to confirm this.

DRUG DOSAGE ASSAY

Materials and Methods

Purification of resting CD4 T cells from peripheral blood

Blood from healthy student donors was obtained through the George Mason University Student Health Center. A primary round of purification utilizing anti CD14, CD56, HLA-DR, HLA-DP and HLA-DQ antibodies (BD Biosciences) was followed by a second round of purification with anti CD8, CD11b and CD19 antibodies (BD Biosciences). Pan mouse IgG Dynabeads from Life Technologies were used to pull out primary antibody-bound cells.

Cell culture

Purified Resting CD4 T cells were cultured in RPMI (Life Technologies) supplemented with 10% fetal bovine serum (Life Technologies), 100 U/mL penicillin and 100 µg/mL streptomycin starting on the day of purification and incubated at 37 °C and 5% CO_2. Cells were cultured in 2ng/mL IL-7 for three days before being infected on the day four.

Infection

Volumes of drug or DMSO were added to aliquots of 1e6 cells in 1mL of RPMI for final drug concentrations of 50µM, 10 µM, 2 µM, 400nM, 80 nM, or DMSO only. One hour after drug addition, cells were pelleted at 300xg for 5 minutes, supernatant was discarded and cells were resuspended in residual media. 200 µL (approximately 250 ng) of vNL4-3 wild type virus was added to each tube along with 2 µL of 100X drug or DMSO to achieve the previously stated final concentrations in solution. These cultures

were then incubated at 37 °C and 5% CO2 for two hours. Cell cultures were then washed twice with 3mL serum-free RPMI (Life Technologies) and resuspended in 1 mL of RPMI+10%FBS. Penicillin (100 U/mL) and streptomycin (100 µg/mL) (Life Technologies) were then added to these cultures along with 10µL of drug dilution or DMSO to achieve the stated concentrations. Day 0 samples were then collected at this time.

p24 ELISA

p24 release was quantified using a PerkinElmer alliance p24 antigen ELISA kit (Perkins Elmer Life Sciences). 150 µL of cell culture was pelleted and 135 µL of the resultant supernatant was lysed and stored at -20°C. p24 samples were harvested at days 0, 1, 3, 5, 6, 7, 8, 9, 10, and 11. IL-7 was maintained at a concentration of 2ng/mL until day 5. Drug concentrations were maintained by adding 10 µL of diluted drug to the appropriate final concentration every 2 days. Results were read using an ELx808 automatic microplate reader (Bio-Tek Instruments) at 630 nm.

Activation

Cells were activated on day 5 by adding anti CD3/CD28 antibody-conjugated Dynabeads (Life Technologies) to the cell cultures at a concentration of 4 beads per cell. To conjugate antibodies to the magnetic beads, a total of 10µg of antibodies were incubated with $4e^8$ Dynabeads for 30 minutes at room temperature. Magnetic beads were then washed with 0.5% BSA-PBS and resuspended in 1mL of 0.5% BSA-PBS.

Results

Resting T cells were isolated from a healthy donor, treated with one of a set of serial drug dilutions, and infected with wild-type, vNL4-3 virus. Viral replication was monitored via sample collection of the culture supernatant over the following weeks. Samples were lysed and analyzed for the viral protein, p24. p24 makes up the capsid of HIV, which encloses and protects the viral genome [47]. The presence of viral capsid in the culture media can therefore be used as a proxy for viral replication. This study should more accurately model the treatment regimen in a typical *in vivo* target than the previous time of addition study. The activation of these cells with CD3/CD28 beads also helps model the likely infection environment, yet other cytokines and cell surface molecules found *in vivo* are likely to further shape the viral life cycle in ways not modelled by this assay.

Cells treated with the highest concentrations of drug used in this assay (50 µM and 10 µM) showed lower p24 release compared to the DMSO treated control (Figure 8). 50µM drug treatment inhibited over 70% of viral replication from day 6 to day 11 post infection. Maximal inhibition (86.6%) was observed on day 11 post infection. Similarly, the 10 µM drug treatment inhibited as much as 59% of viral replication by day 11. Both the 50 µM and the 10 µM drug treatments inhibited viral replication steadily throughout this time period. Of note, the p24 concentration in the 50 µM treated group on day 11 (479 pg/mL) was the close to that found in day 1 samples for the same group (439 pg/mL). The inhibition observed at 50 µM dosage was somewhat higher than what was typically observed in previous time of addition assays. This is likely due to the fact that the p24 ELISA was carried out longer than the time of addition experiment which was

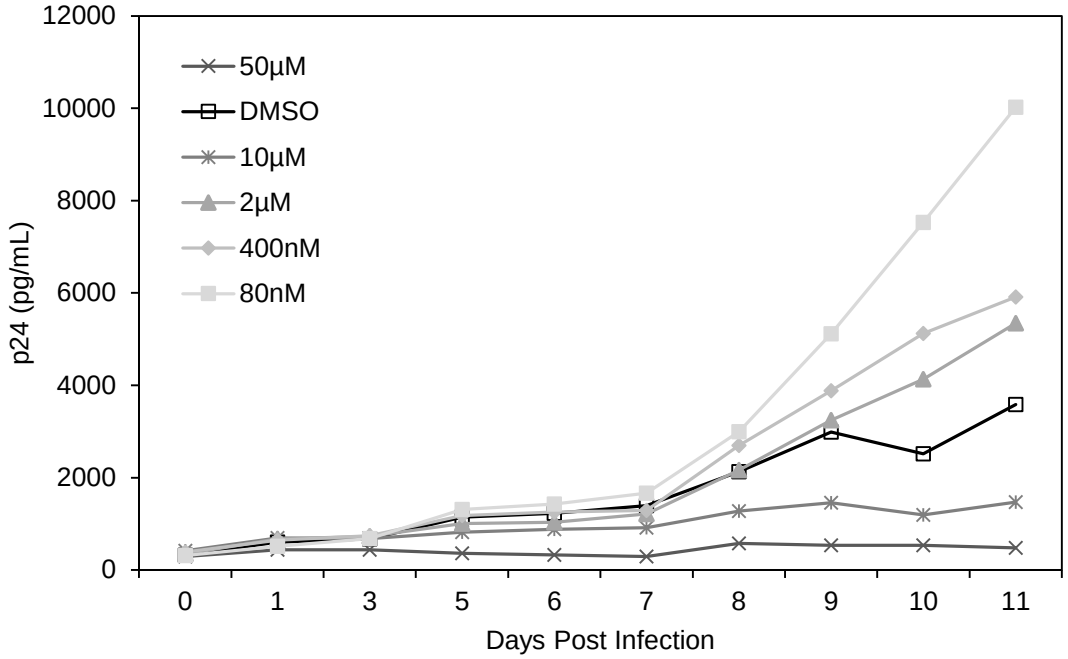

Figure 8. NSC 156594 inhibits HIV-1 replication at high dosages.

Resting CD4 T cells were purified from the blood of a single donor, and pretreated with NSC 156594 at the indicated concentrations for 1 hour before infection. Drug concentrations were maintained in culture throughout the course of the experiment.

assayed 2-3 days post infection at the latest. This assay therefore likely provides a better estimate of the efficacy of this concentration *in vivo* than the previous time of addition studies.

Interestingly, cells treated with lower concentrations of drug (2 µM, 400 nM, 80 nM) exhibited enhanced p24 release compared to the DMSO-treated control. In the 80 nM treated sample, enhancement of viral replication was close to 200% at day 10. The 2 µM and 400 nM drug treatment groups enhanced viral replication up to 64% and 104%, respectively. The cause of this enhancement of replication is unclear at the moment but could possibly result from both inhibitory and stimulatory pathways targeted by this drug acting in opposition to each and having different IC50s. Regardless, this potential for enhancement is a serious concern and will need to be clarified before significant work is done with this drug.

A3G PATHWAY

Background

HIV Vif is an accessory protein that plays several roles during infection. One of the most significant is the degradation of the host restriction factor A3G. In the absence of Vif, A3G is incorporated into budding viruses and interferes with viral replication during the subsequent round of replication [38]. The primary mechanism by which A3G restricts viral replication is thought to be hypermutation of the newly formed cDNA during and after reverse transcription of the viral genome [48].

Cells that support HIV-1 infection can be further categorized based on their ability to restrict the replication of Vif deficient viruses. This trait can be traced to the expression or non-expression of appreciable levels of the APOBEC family of host restriction factors. H9 cells are described as non-permissive, meaning that they do not permit the replication of Vif deficient viruses. As expected, H9 cells express high levels of A3G [49]. In contrast, CEM-SS cells are permissive and significant quantities of virus can be obtained from Vif deficient HIV strains. It is worth noting that although some have raised concern over the activity of endogenous H9-derived A3G [50], H9 cells infected with *vif* mutant viruses contain A3G with more activity than those associated with wild type virus [51]. Others have found significantly increased G to A mutation rates of viral DNA in H9 cells infected with Vif-deficient viruses. In these cases, the G to A mutation rate was 100% higher when Vif-deficient virus was used. Additionally, these occurred in specific sequence contexts indicative of A3G and A3F (GG and GA dinucleotides), further confirming the role of A3G activity in this cell line [52]. Our choice of H9 cells for

this assay is then appropriate, as this indicates H9 cells respond differentially to HIV infection based on the functionality of the Vif-A3G interaction.

Because of the evidence we had found in relevant literature, we wanted to investigate any role A3G may play in the inhibition exerted by this drug. We hypothesized that if NSC 156594 acts in part by inhibiting the degradation of A3G, our drug should exert less inhibition on viral replication in cells which do not express A3G compared to those which do. It was important that this study be done as a comparison of *relative* inhibition between the two cell types as the basal levels of HIV replication in each were likely to be different.

Materials and Methods

Cell culture

$1e^6$ CEM-SS cells were aliquoted into 2, 5mL tubes. Likewise, $1e^6$ H9 cells were aliquoted into 2, 5mL tubes. One tube of each cell type was pre-treated with 50μM NSC 156594 for 1 hour before infection. Similarly, one tube of each cell type was pre-treated with an equal volume of DMSO as a control.

Infection

All 4 cell aliquots were infected with approximately 200-250ng of wild type, vNL4-3 via spinoculation. Infections were centrifuged at 300xg for 2 hours. After the centrifugation, all infections were washed twice with RPMI+10%FBS and resuspended in 1mL RPMI supplemented with 10% FBS (Life Technologies), penicillin (100 U/ml) and streptomycin (100 μg/mL) (Life Technologies).

Sample collection

Day 0 samples were collected immediately after post infection resuspension. Afterwards, a full volume of drug was added to maintain drug concentration every 2 days. p24 release was quantified using a PerkinElmer alliance p24 antigen ELISA kit (Perkins Elmer Life Sciences). 150 µL of cell culture was pelleted, and 135 µL of resultant supernatant was lysed in 15 µL of p24 ELISA lysis buffer. Samples were then stored at -20°C. p24 samples were harvested at days 0, 1, 2, 3, 4, 5, 6, 7, 8 and 9 post infection. 500 mL of growth media was changed out after harvests early in the time course. Later, 150µL of media was changed out after each harvest. Results were read using an ELx808 automatic microplate reader (Bio-Tek Instruments) at 630 nm.

Results

Starting at day 3 post infection onward, there was a very apparent difference in the inhibition profiles between the two cell lines. After infection, H9 cells showed a significant reduction in p24 release in the presence of NSC 156594. In stark contrast to this, CEM-SS cells showed only a modest inhibition of viral replication in the presence of the drug (data not shown). Although the raw data for H9+Drug treated samples were well within the dynamic range of this assay, the other sample groups reached high p24 concentrations that were out of reliable detection range, and we suspected they may not show the full degree of the replicative differences in the two cell types. To confirm these results we repeated the p24 with the same set of lysates but used greater dilutions to detect higher concentrations.

Upon diluting the samples, we observed the same relative level of H9+drug p24 concentrations, but much higher replication of the other 3 sample groups (Figure 9). H9+drug samples remained at levels < 3000 pg/mL, but the H9+DMSO contained p24 levels > 150,000 pg/mL. The two cell types indeed showed different levels of basal replication; DMSO-treated H9 cell cultures had similar maximal p24 concentrations to the drug-treated CEM-SS samples. Also, the H9 control lagged behind the CEM-SS control in terms of the onset of viral replication, being delayed by a day or more. Again, the cell types showed very different inhibition profiles, with H9 cells responding very dramatically upon drug treatment. CEM-SS cells experienced some inhibition of viral replication but the inhibition was much weaker than that in the H9 culture. Plotting the data on a log scale shows the true extent of inhibition in H9+drug culture (Figure 10).

As Figure 11 shows, levels of viral replication were similar for the first 2 days after infection, but over time the drug-treated H9 samples showed progressively less replicative capacity. From day 5 to day 9, drug treated H9 cultures only showed 1-2% as much p24 release as the DMSO-treated H9 control, whereas the CEM-SS group ranged from 61% to 75% of the control over the same time period.

The dramatic inhibition in H9 cells suggest that the drug may be able to inhibit the degradation of A3G this cell type. In the CEM-SS cells, no A3G is present, and the drug cannot act on this target. As there is still observable inhibition in CEM-SS cells, it is possible that the drug may also be acting at a transcriptional level as previously hypothesized. These data seem to support the possibility of two modes of action for this drug. The observed inhibition in CEM-SS cells was not as dramatic as the earlier findings

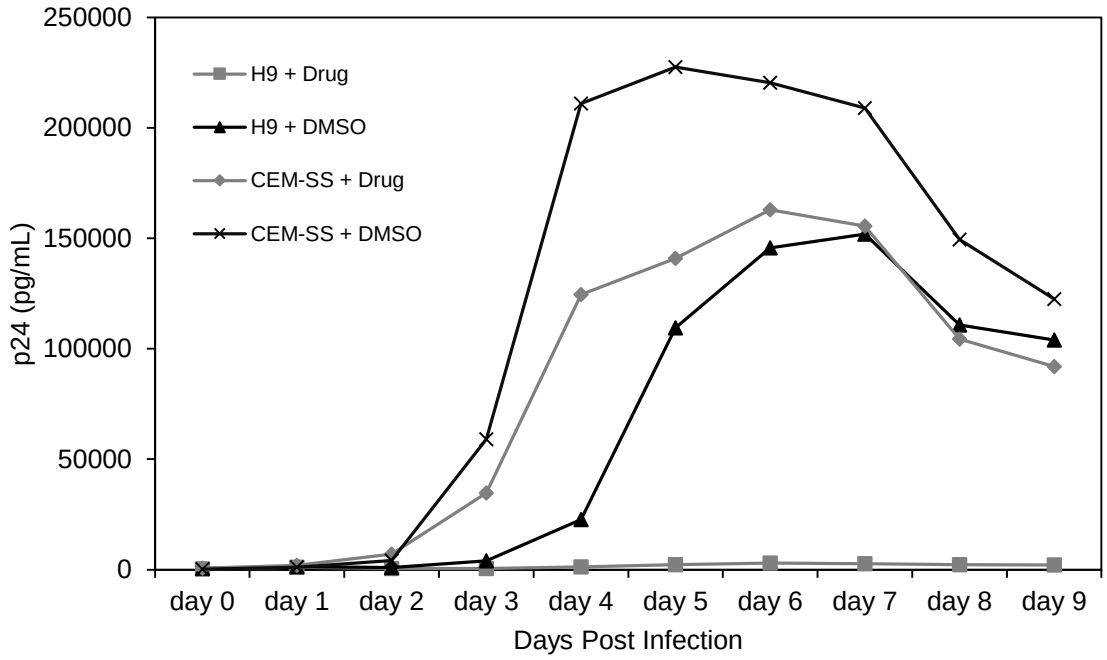

Figure 9. NSC 156594 differentially effects replication in H9 and CEM-SS cells.

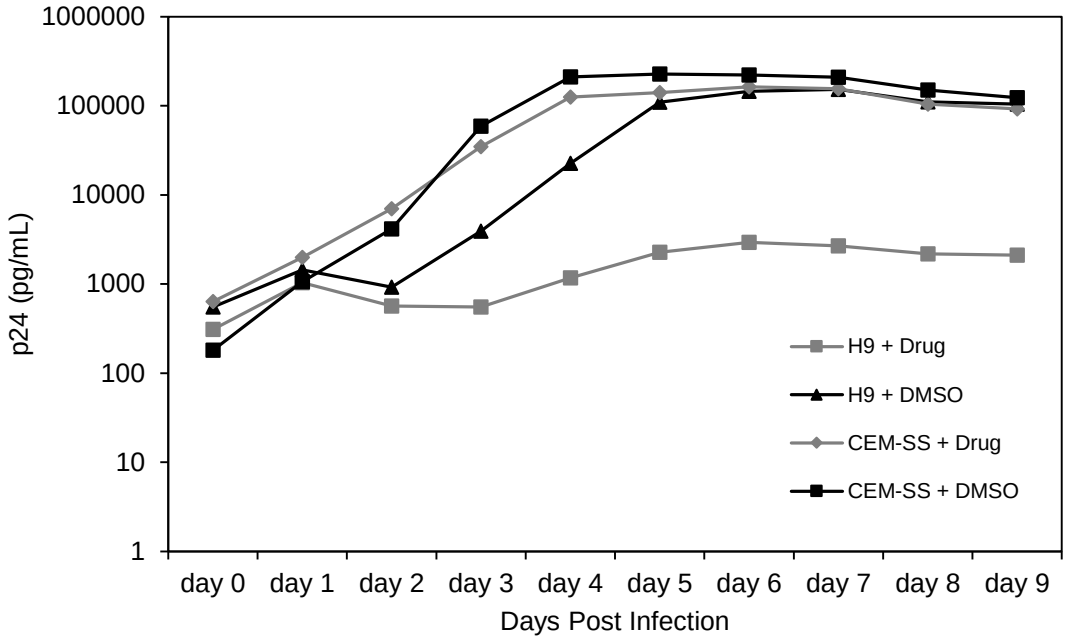

Figure 10. NSC 156594 differentially effects viral replication in H9 and CEM-SS cells.

A

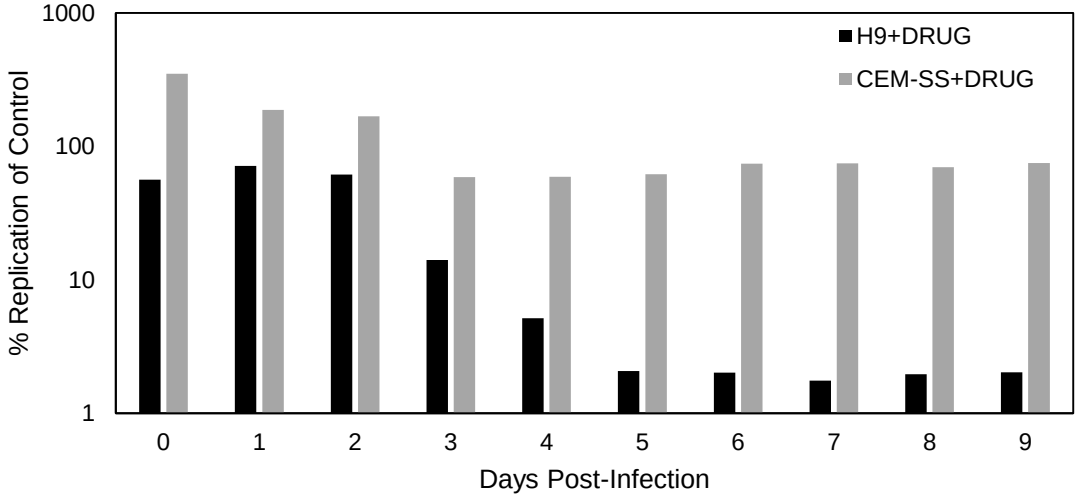
1000
100
10
1
% Replication of Control
H9+DRUG
CEM-SS+DRUG
0
1
2
3
4
5
6
7
8
9
Days Post-Infection

B

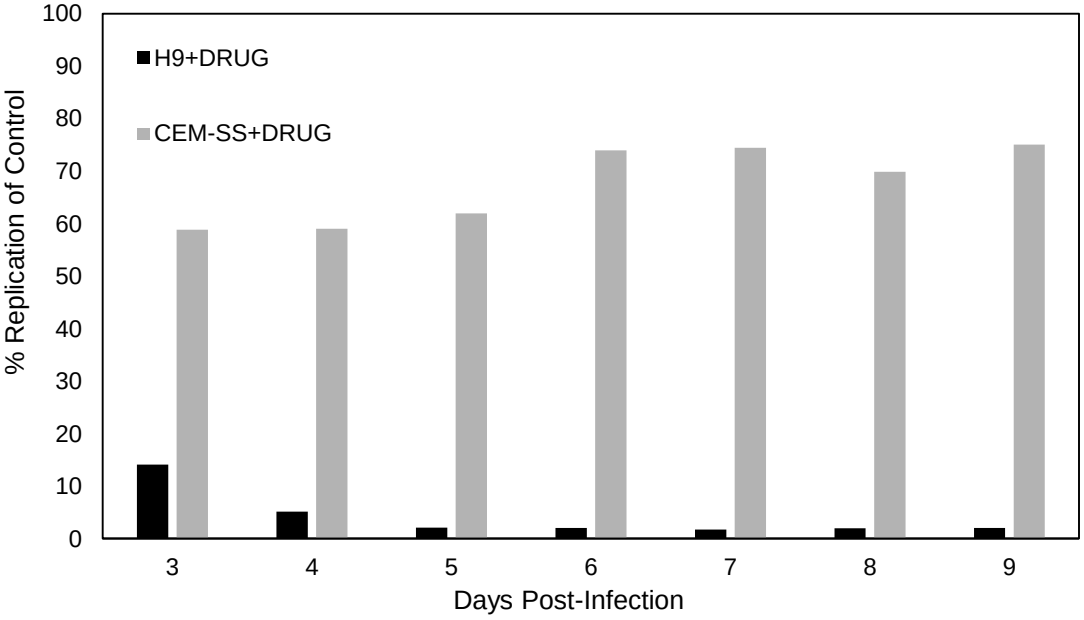
100
90
80
70
60
50
40
30
20
10
0
% Replication of Control
H9+DRUG
CEM-SS+DRUG
3
4
5
6
7
8
9
Days Post-Infection

Figure 11. Relative inhibition due to drug treatment.

Panel A shows relative levels of viral replication plotted on a log scale and normalized to the p24 conentration of the corresponding DMSO-treated time point. Panel B shows later time points in the same set of data also normalized to the respective DMSO-treated controls.

in our CEM-SS-based CloneX cell line. When infected in the presence of this drug, CloneX cells do not produce high levels of virus. The inhibition in these early time points can be as great as 66%. In contrast, the CEM-SS cells in this assay showed lower levels of inhibition in the presence of the drug during later time points in the assay. This may be due to the fact that the earlier flow cytometry based assay only analyzes the effect of the drug 2-3 days post infection, whereas the p24 ELISA detects the cumulative effects of over a week of replication. Indeed, inhibition of up to 41% can be seen in the drug-treated CEM-SS sample on days early in time course. The main usefulness of this experiment lies in its ability to inform us on the role of APOBEC3G in the inhibition this drug exerts. Usefulness of the drug *in vivo* will likely be more similar to the drug concentration study performed in resting T cells.

LTR TRANSCRIPTION

Materials and Methods

Reporter construct

A *tat-IRES* insert was cloned from the plasmid pNL-tat-IRES-GFP via PCR amplification incorporating EcoR1 sites, and inserted into the recipient pNL-luc plasmid. The pNL-tat-IRES-Luc construct is a lentiviral-based plasmid which expresses functional HIV-1 Tat and Firefly Luciferase. As more Tat is produced by basal LTR driven transcription, it transactivates the LTR promoter by binding to the transcriptional activation region (TAR) of nascent mRNAs and recruiting cellular transcription factors to hyperphosphorylate RNA Polymerase II. This leads to increased synthesis of transcripts under the control of the LTR, including the luciferase reporter gene. Any interference with Tat's ability to transactivate transcription results in diminished reporter transcript synthesis protein production

Cell culture and transfection

HEK 293T cells were cultured at 37°C and 5% CO_2, supplemented with penicillin (100 U/mL) and streptomycin (100 µg/mL) (Life Technologies). Cells were grown to approximately 70% confluency and then used to seed a 6 well plate. $5e^5$ cells were seeded into each well one day before the transfection, then cultured for 24 hours. The next day, 4µg of plasmid per well was transfected according to Life Technologies' Lipofectamine 2000 protocol. After the transfection, cells were cultured for 5.5 hours before changing out serum free DMEM (Life Technologies) for DMEM + 10% FBS (Life Technologies).

One day after transfection, cells were trypsinized with TryPle Express (Life Technologies), and half the cells were removed. 2 mL of fresh media was added along with 20µL of 100X working stock of the drug. Final concentrations of drug in the culture were 50µM, 10µM, 2 µM, and 400 nM. 20µL of DMSO was added to an additional well as a negative control.

Analysis

Two days after transfection, cells were trypsinized and resuspended in DMEM+10% FBS. 1/3 of the cells were then removed for analysis. Drug or DMSO was added back to the cultures. Aliquoted cells were pelleted and subsequently lysed in luciferase lysis reagent (Promega). Lysate was added to a 96 well plate and analyzed via a GloMax-Multi luminometer (Promega). Each well was read 3 times. Three days after transfection, the remaining cultures were trypsinized, $1.18e^5$ cells were removed from each culture, and analyzed according to the previously described protocol with serial dilutions for each sample made using lysis buffer as diluent.

Results

Based on our findings from the *nef* transcript assay, we expected to see an obvious inhibition of Tat-mediated reporter transcription. Surprisingly, drug treatment enhanced reporter activity, suggesting an increase in Tat-mediated LTR transcription. The 50µM treated sample exhibited an over 100% increase in reporter activity. All drug treatment groups showed reporter activity at least 100% higher than the DMSO – treated control. A point of concern with these results was relatively high RLUs, reaching as high as 10^9. To determine whether we had observed the full effect of the drug, and not

just saturated the machine, the analysis was repeated the next day, this time with equal numbers of cells for each sample and using a dilution set to ensure values were within the dynamic range of our machine.

Similar patterns were observed in the undiluted sample the second day, with high RLUs and over 100% enhancement in every sample. Dilution of the sample lysates yielded lower RLUs which could be reliably assayed by our luminometer (Figure 12). In these samples, enhancement was still seen but was less dramatic than in the undiluted set. Samples in the 1:10 dilution set ranged from 33-62% enhancement based on the DMSO-treated control. Similarly, samples in the 1:100 dilution set ranged from 25-63% enhancement, with no obvious dosage dependence (Figure 13).

The enhancement seen in the 1:10 and 1:100 diluted samples are likely to be indicative of the actual enhancement of expression and activity. The RLU values in the diluted samples were located further from the upper limits of the dynamic range of our machine, and the enhancement seen in the two dilution sets of samples were highly similar to each other, providing another indicator of their accuracy.

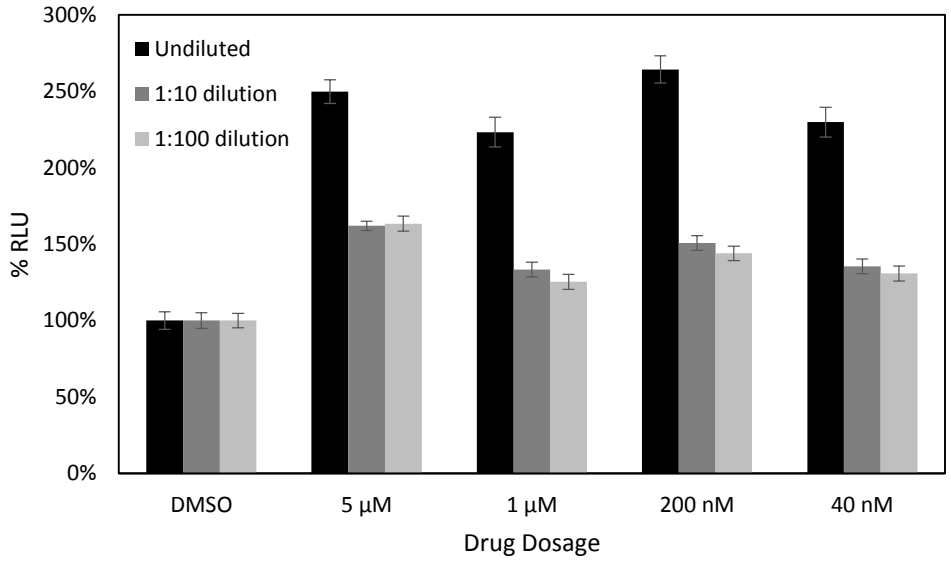

Figure 12. NSC 156594 stimulates LTR-driven transcription.

$1.18e^5$ cells from culture were lysed and analyzed for LTR-driven luciferase activity as described previously. Serial dilutions were made from each lysate sample to ensure results were within the dynamic range of our luminometer. Results shown are averages of 3 reads of the same plate of lysate samples, normalized to the respective DMSO control.

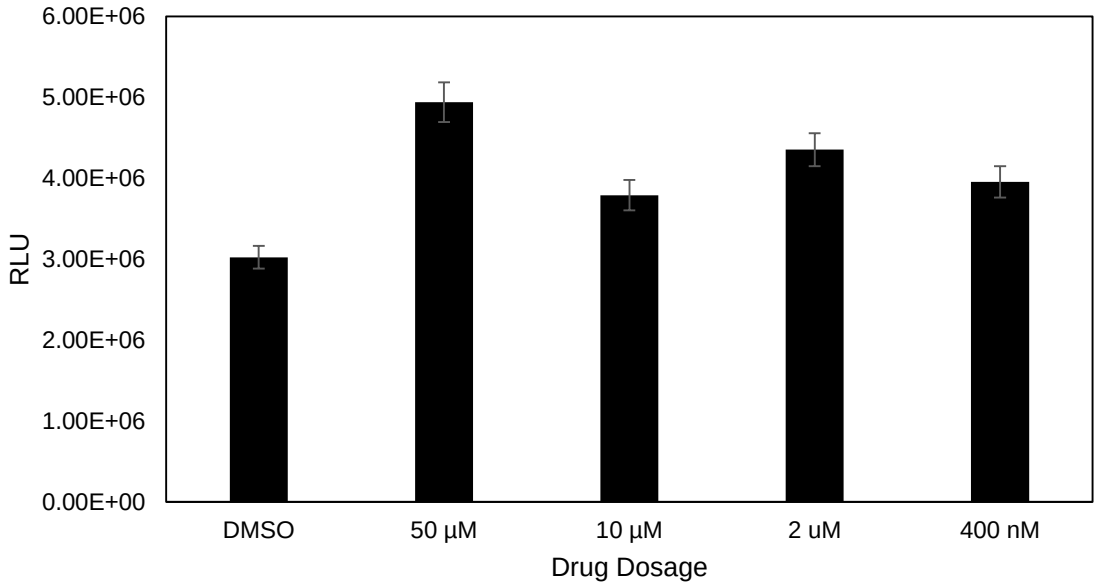

Figure 13. NSC 156594 stimulates LTR-driven transcription.

1.18e^5 cells from culture were lysed and analyzed for LTR-driven *luc* transcription as described previously. Shown are the data from the 1:100 dilution set. Results shown are averages of 3 reads of the same plate of lysate samples.

CONCLUSION

NSC 156594 exerts maximal inhibition at early time points

Maximal inhibition of viral replication in our CEM-SS based reporter cell line was 58% without spinoculation and 66% when cells were spinoculated at 600 x g, which occurred at 6 hours pre-infection and 1 hour pre-infection, respectively. These results prompted us to investigate the effect of this drug on early to mid stages of the viral life cycle, although they do not exclude the possibility that later time points could also be effected. *In vivo* relevance from these experiments is limited due the usage of an immortal, CEM-SS based line.

NSC 156594 may target *nef* transcription

Entry was not tested specifically, but results from subsequent experiments indicated the drug did not act on this stage: inhibition of total DNA and 2-LTR synthesis due to the drug was negligible. Although it could not be tested directly, cDNA integration is also unlikely to be a target of this drug as evidenced by a lack of differential 2-LTR circle copy number. *Nef* transcripts, however, were markedly reduced in the drug treated group by as much as 70% at 24 hours post infection and 50% at 48 hours post infection. *In vivo* relevance is still limited as CEM-SS cells were used for this study as well. Additionally, this experiment used single cycle virus and as such, could not detect most of the effects of a possible A3G mechanism.

Drug treatment exerts dosage-dependent effects on p24 release

For a better understanding of *in vivo* relevance, primary resting T cells were used for our drug dosage assay. Enhancement of viral replication was seen at lower concentrations, but higher concentrations of 50 µM and 10 µM showed good levels of inhibition of p24 release compared to the DMSO-treated control (86% and 59% inhibition, respectively). Of note, 50 µM treatment inhibited over 70% of viral replication for the entire second half of the time course. This further supports the use of a concentration of 50 µM for subsequent experiments, rather than lower dosages. Low dosages of 2 µM, 400 nM, and 80 nM, in fact, enhance viral p24 release, with near 200% enhancement seen by the end of the time course in the 80 nM drug-treated sample. Results here are more representative of the setting *in vivo*, and would likely reflect any transcriptional inhibition as well as A3G-based inhibition, as it has been shown that A3G can restrict viral replication in activated Th1 cells [53].

The observed pattern of enhancement of viral replication at low dose drug treatments is not ideal for a candidate drug. Factors such as uneven uptake into different tissues, lag periods before equilibrium is achieved, and differing rates of elimination mean drugs are often present in the body at concentrations other than that desired. This drug in its present form may therefore not be suited for routine, chronic usage. It is possible it may be adapted or chemically synthesized in a way to minimize these effects. As the cell type used in this assay was primary resting T cells from a blood donor, there is always a small chance that the donor specific variations may be responsible for some of the observed data. While this is unlikely to account for any large patterns seen in the presented data, it would

still be wise to repeat this experiment in two other donors at minimum to clarify the extent of donor to donor genetic and metabolic variation.

NSC 156594 may inhibitA3G degradation

While the results from the H9/CEM-SS comparative study may not provide the most accurate reflection of the extent of *in vivo* inhibition, they do provide an indication of the nature of inhibition which may be occurring upon drug treatment. At first glance, the comparative study seems to suggest that the differences seen in HIV replication between drug-treated samples of the two groups is a result of differing expression levels of A3G. Other possibilities exist as to the difference in replicative potential between the cell types. Because A3G levels are different between the two cell types, we know *a priori* that there are different transcriptional or metabolic networks active in the two cell types. If transcriptional differences are driving the different levels of A3G, there could also be differences in transcription of the HIV provirus that may skew the interpretation of the data. If this is the case it would be unclear as to whether the drug may exert more inhibition in H9 cells due to greater access to transcriptional complex machinery.

To address this question, we have begun creating VSV-G pseudotyped lentiviral particles containing an A3G expression vector. We intend to transduce CEM-SS cells with this construct for a stable integration and subsequent expression of A3G. Once this cell line is established, a direct comparison could be made with CEM-SS upon drug treatment and infection.

Drug treatment enhances Tat-mediated, LTR-driven transcription

The LTR transfection study showed enhanced Tat-mediated, LTR-based transcription upon drug treatment at dosages of 50µM, 10µM, 2µM, and 400 nM. Drug-stimulated enhancement at these dosages ranged from 25-63%. No dosage dependent effects were observed, as the enhancement of reporter function appeared to be fairly stable across diminishing concentrations of drug treatment. This may indicate that any potential stimulatory activity of this drug has an EC50 well below that of the concentrations used in this experiment. If there is indeed a stimulatory target of the drug, it is possible that it is saturated at drug levels below 40nM. Additionally, as there was no transfection control for this experiment, it is possible that differing transfection efficiencies could cause the observed results. The repetition of this experiment via a dual transfection with 2 different luciferase reporters would clarify this possibility. Furthermore, it is worth considering that cytokine environments in secondary lymphoid tissue may induce even higher transcriptional levels than those observed in this study. This could synergize with low drug dosage to induce enhanced proviral transcription *in vivo*. The effects of this drug on transcription are therefore a high priority for future investigation.

Some research suggests that drugs which target the interaction of CBF-β and RUNX1 may result in activation of the HIV-1 provirus from latency. A study by Klase et al. show that over-expression of CBF-β and RUNX1 reduces the synthesis of viral proteins [54]. This study used CBF-β and RUNX1 expression vectors transfected into 293T

cells, the same cell type used in the present study. Cotransfection of the two expression vectors resulted in over 60% inhibition of LTR driven luciferase reporter, but not CMV or EF1 promoter based reporters [54]. Further support of this pathway is the identification of several well-conserved RUNX1 binding sites in the HIV-1 LTR [54]. Finally, the addition of a RUNX1- CBF- β binding inhibitor synergizes with the established histone deacetylase (HDAC) inhibitor, suberoylanilide hydroxamic acid (SAHA) to reactivate latent HIV-1 provirus [54]. The RUNX1- CBF- β binding inhibitor which was used, Ro5-3335, is strikingly similar in structure to NSC 156594, differing only in the presence of a single methyl group.

To obtain a better picture of what may be happening with the observed transcriptional enhancement, we would like to perform the same experiment in a more relevant cell type. As there are likely different signaling pathways active in the natural targets of the virus, we would like to use CEM-SS cells in a similar study. To this end, we have constructed VSV-G pseudotyped lentiviral particles containing the pNL-Tat-IRES-Luc plasmid, which will be used to transduce CEM-SS cells. Alternatively, it would also be possible to accomplish the same goal through the transfection of CEM-SS cells directly with this construct. RUNX1 is also likely to have additional transcriptional relevance in CEM-SS cells as it has been shown to control T cell lineage determination [55], and chromosomal aberrations involving the RUNX1 gene often are responsible for the development of leukemia [56]. As such, the use of CEM-SS cells would be a significant improvement to the study design.

Remaining questions

Any potential for drug dosages to enhance viral replication needs to be clarified before further work is done. The reason both inhibitory and stimulatory profiles were observed remains unclear. It is possible that the enhancement of viral p24 release seen in low dosage drug treatments could be due to the observed stimulation of LTR-based transcription. Enhancement of transcription was seen in every drug dosage including 50 µM and 10 µM, yet the 50 µM and 10 µM treatment in the drug dosage assay showed inhibition of viral replication. It is possible that multiple drug pathways are acting in opposition to each other which have different EC50s. Further complicating this interpretation of the data is the observed inhibition of *nef* transcription, a study which will need to be repeated before further conclusions can be drawn.

One of the largest issues requiring attention is the lack of data replication. Many of the experiments performed in this study build upon and support the conclusions of those which precede it. Despite this, most of the experiments done in the current study have only been performed once, and as such, are a possible source of error without repeated confirmation. Data from total DNA synthesis, 2-LTR circle synthesis, *nef* transcript synthesis, and the drug dosage study are the primary experiments which require replication. Experiments which analyze LTR transcription and the A3G pathway will be addressed and thus replicated via other experiments which improve upon the original study designs.

Enhancement at low drug dosages may limit the application of the current compound under study, but our lab has identified other CBF-β – RUNX1 inhibitors for

possible investigation, and further characterization of NSC 156594 could be useful in modeling the efficacy of this class of drugs as a whole. This avenue would be worth pursuing if NSC 156594 does prove to act, at least in part, by interfering with Vif-mediated A3G degradation, as this is a relatively underexploited pathway for HIV therapeutics.

Should the current conclusions prove to be accurate, the stimulatory potential of this drug could be useful for purposes other than suppressing viral load. Recently, significant attention has shifted to shock and kill therapy, a process which relies on the reactivation of latent, and immunologically silent, provirus to purge viral reservoirs. After reactivation, infected cells ostensibly die through immune mechanisms or virus-mediated cell toxicity, and newly produced virions are blocked via simultaneous administration of antiretrovirals [57]. If NSC 156594 does enhance LTR-driven transcription, it could potentially be used for this purpose. The related inhibitor, Ro5-3335, is being investigated specifically for this purpose, and could be an indicator of the usefulness of NSC 156594 for this purpose.

REFERENCES

1. World Health Organization. *Global update on the health sector response to HIV, 2014*. (World Health Organization, 2014). at <http://apps.who.int//iris/handle/10665/128494>

2. World Health Organization. *World health statistics 2014*. (World Health Organization, 2014). at http://apps.who.int/iris/bitstream/10665/112738/1/9789240692671_eng.pdf?ua=1

3. Dixon, S., McDonald, S. & Roberts, J. The impact of HIV and AIDS on Africa's economic development. *BMJ* **324,** 232–234 (2002).

4. Kidman, R. & Thurman, T. R. Caregiver burden among adults caring for orphaned children in rural South Africa. *Vulnerable Child. Youth Stud.* **9,** 234–246 (2014).

5. World Health Organization. *A guide to monitoring and evaluation for collaborative TB/HIV activities*. (World Health Organization, 2015). at http://apps.who.int/iris/bitstream/10665/150627/1/9789241508278_eng.pdf?ua=1&ua=1

6. Coleman, C. M. & Wu, L. HIV interactions with monocytes and dendritic cells: viral latency and reservoirs. *Retrovirology* **6,** 51 (2009).

7. Crowe, N. Y., Godfrey, D. I. & Baxter, A. G. Natural killer T cells are targets for human immunodeficiency virus infection. *Immunology* **108,** 1–2 (2003).

8. Grossman, Z., Meier-Schellersheim, M., Paul, W. E. & Picker, L. J. Pathogenesis of HIV infection: what the virus spares is as important as what it destroys. *Nat. Med.* **12,** 289–295 (2006).

9. Spear, M., Guo, J. & Wu, Y. The trinity of the cortical actin in the initiation of HIV-1 infection. *Retrovirology* **9,** 45 (2012).

10. Zhou, Y., Zhang, H., Siliciano, J. D. & Siliciano, R. F. Kinetics of Human Immunodeficiency Virus Type 1 Decay following Entry into Resting CD4+ T Cells. *J. Virol.* **79,** 2199–2210 (2005).

11. Mehandru, S. *et al.* Primary HIV-1 Infection Is Associated with Preferential Depletion of CD4+ T Lymphocytes from Effector Sites in the Gastrointestinal Tract. *J. Exp. Med.* **200,** 761–770 (2004).

12. Alizon, S. & Magnus, C. Modelling the course of an HIV infection: insights from ecology and evolution. *Viruses* **4,** 1984–2013 (2012).

13. McGary, C. S. *et al.* Increased stability and limited proliferation of CD4+ central memory T cells differentiate non-progressive SIV-infection of sooty mangabeys from progressive SIV-infection of rhesus macaques. *J. Virol.* JVI.03515–13 (2014). doi:10.1128/JVI.03515-13

14. Liu, Z. *et al.* Elevated relative fluorescence intensity of CD38 antigen expression on CD8+ T cells is a marker of poor prognosis in HIV infection: results of 6 years of follow-up. *Cytometry* **26,** 1–7 (1996).

15. Hunt, P. W. *et al.* T Cell Activation Is Associated with Lower CD4+ T Cell Gains in Human Immunodeficiency Virus-Infected Patients with Sustained Viral Suppression during Antiretroviral Therapy. *J. Infect. Dis.* **187,** 1534–1543 (2003).

16. Oxenius, A. *et al.* Early highly active antiretroviral therapy for acute HIV-1 infection preserves immune function of CD8+ and CD4+ T lymphocytes. *Proc. Natl. Acad. Sci. U. S. A.* **97,** 3382–3387 (2000).

17. Kulpa, D. A. *et al.* The immunological synapse: the gateway to the HIV reservoir. *Immunol. Rev.* **254,** 305–325 (2013).

18. May, M. *et al.* Impact of late diagnosis and treatment on life expectancy in people with HIV-1: UK Collaborative HIV Cohort (UK CHIC) Study. *BMJ* **343,** d6016–d6016 (2011).

19. Moore, R. D. & Chaisson, R. E. Natural history of HIV infection in the era of combination antiretroviral therapy. *AIDS Lond. Engl.* **13,** 1933–1942 (1999).

20. Department of Health and Human Services. *Update: Trends in AIDS Incidence -- United States, 1996*. 861–867 (Centers for Disease Control and Prevention, 1997).

21. UNAIDS. *Access to Antiretroviral Therapy in Africa*. (UNAIDS, 2013). at <http://www.unaids.org/sites/default/files/media_asset/20131219_AccessARTAfricaStatusReportProgresstowards2015Targets_en_0.pdf>

22. Bor, J., Herbst, A. J., Newell, M.-L. & Bärnighausen, T. Increases in Adult Life Expectancy in Rural South Africa: Valuing the Scale-Up of HIV Treatment. *Science* **339,** 961–965 (2013).

23. Department of Health and Human Services. *Guidelines for the use of antiretroviral agents in HIV-1-infected adults and adolescents*. (Department of Health and Human Services, 2013). at http://aidsinfo.nih.gov/contentfiles/lvguidelines/adultandadolescentgl.pdf

24. World Health Organization. *The WHO consolidated guidelines on the use of antiretroviral drugs for treating and preventing HIV infection*. (World Health Organization, 2013). at <http://apps.who.int//iris/handle/10665/94189>

25. Prendergast, A. J., Essajee, S. & Penazzato, M. HIV and the Millennium Development Goals. *Arch. Dis. Child.* **100 Suppl 1,** S48–52 (2015).

26. Calvo, K. R. & Daar, E. S. Antiretroviral Therapy: Treatment-experienced Individuals. *Infect. Dis. Clin. North Am.* **28,** 439–456 (2014).

27. World Health Organization. *The HIV drug resistance report - 2012*. (World Health Organization, 2012). at http://apps.who.int/iris/bitstream/10665/75183/1/9789241503938_eng.pdf

28. Karn, J. & Stoltzfus, C. M. Transcriptional and Posttranscriptional Regulation of HIV-1 Gene Expression. *Cold Spring Harb. Perspect. Med.* **2,** (2012).

29. Burnett, J. C., Miller-Jensen, K., Shah, P. S., Arkin, A. P. & Schaffer, D. V. Control of stochastic gene expression by host factors at the HIV promoter. *PLoS Pathog.* **5,** e1000260 (2009).

30. Ott, M., Geyer, M. & Zhou, Q. The Control of HIV Transcription: Keeping RNA Polymerase II on Track. *Cell Host Microbe* **10,** 426–435 (2011).

31. Isel, C. & Karn, J. Direct evidence that HIV-1 Tat stimulates RNA polymerase II carboxyl-terminal domain hyperphosphorylation during transcriptional elongation. *J. Mol. Biol.* **290,** 929–941 (1999).

32. Zhang, W., Du, J., Evans, S. L., Yu, Y. & Yu, X.-F. T-cell differentiation factor CBF-β regulates HIV-1 Vif-mediated evasion of host restriction. *Nature* **481,** 376–379 (2012).

33. Adya, N., Stacy, T., Speck, N. A. & Liu, P. P. The Leukemic Protein Core Binding Factor β (CBFβ)–Smooth-Muscle Myosin Heavy Chain Sequesters CBFα2 into Cytoskeletal Filaments and Aggregates. *Mol. Cell. Biol.* **18,** 7432–7443 (1998).

34. Jager, S. *et al.* Vif hijacks CBF - β to degrade APOBEC3G and promote HIV-1 infection. *Nature* **481,** 371–375 (2011).

35. Chang, L.-C. *et al.* APOBEC3G exerts tumor suppressive effects in human hepatocellular carcinoma. *Anticancer. Drugs* **25,** 456–461 (2014).

36. Koyama, T. *et al.* APOBEC3G oligomerization is associated with the inhibition of both Alu and LINE-1 retrotransposition. *PloS One* **8,** e84228 (2013).

37. Arias, J. F., Koyama, T., Kinomoto, M. & Tokunaga, K. Retroelements versus APOBEC3 family members: No great escape from the magnificent seven. *Virology* **3,** 275 (2012).

38. Kim, D. Y. *et al.* CBFβ stabilizes HIV Vif to counteract APOBEC3 at the expense of RUNX1 target gene expression. *Mol. Cell* **49,** 632–644 (2013).

39. National Center for Biotechnology Information. *NCI AIDS Antiviral Assay AID=179*. (National Cancer Institute). at <http://pubchem.ncbi.nlm.nih.gov/assay/assay.cgi?aid=179#aDescription>

40. Weislow, O. S. *et al.* New soluble-formazan assay for HIV-1 cytopathic effects: application to high-flux screening of synthetic and natural products for AIDS-antiviral activity. *J. Natl. Cancer Inst.* **81,** 577–586 (1989).

41. Wu, Y., Beddall, M. H. & Marsh, J. W. Rev-Dependent Indicator T Cell Line. *Curr. HIV Res.* **5,** 394–402 (2007).

42. Guo, J., Wang, W., Yu, D. & Wu, Y. Spinoculation Triggers Dynamic Actin and Cofilin Activity That Facilitates HIV-1 Infection of Transformed and Resting CD4 T Cells. *J. Virol.* **85,** 9824–9833 (2011).

43. O'Brien, W. A. HIV-1 entry and reverse transcription in macrophages. *J. Leukoc. Biol.* **56,** 273–277 (1994).

44. Li, L. *et al.* Role of the non-homologous DNA end joining pathway in the early steps of retroviral infection. *EMBO J.* **20,** 3272–3281 (2001).

45. Mandal, D. & Prasad, V. R. Analysis of 2-LTR circle junctions of viral DNA in infected cells. *Methods Mol. Biol. Clifton NJ* **485,** 73–85 (2009).

46. Friedrich, B., Li, G., Dziuba, N. & Ferguson, M. R. Quantitative PCR used to Assess HIV-1 Integration and 2-LTR Circle Formation in Human Macrophages, Peripheral Blood Lymphocytes and a CD4+ Cell Line. *Virol. J.* **7,** 354 (2010).

47. Pornillos, O., Ganser-Pornillos, B. K. & Yeager, M. Atomic-level modelling of the HIV capsid. *Nature* **469,** 424–427 (2011).

48. Nowarski, R. *et al.* APOBEC3G Inhibits HIV-1 RNA Elongation by Inactivating the Viral Trans-Activation Response Element. *J. Mol. Biol.* **426,** 2840–2853 (2014).

49. Wang, Y., Kinlock, B. L., Shao, Q., Turner, T. M. & Liu, B. HIV-1 Vif inhibits G to A hypermutations catalyzed by virus-encapsidated APOBEC3G to maintain HIV-1 infectivity. *Retrovirology* **11,** (2014).

50. Thielen, B. K. *et al.* T Cells Contain an RNase-Insensitive Inhibitor of APOBEC3G Deaminase Activity. *PLoS Pathog.* **3,** (2007).

51. Britan-Rosich, E., Nowarski, R. & Kotler, M. Multifaceted counter-APOBEC3G mechanisms employed by HIV-1 Vif. *J. Mol. Biol.* **410,** 1065–1076 (2011).

52. Zhou, T., Han, Y., Dang, Y., Wang, X. & Zheng, Y.-H. A novel HIV-1 restriction factor that is biologically distinct from APOBEC3 cytidine deaminases in a human T cell line CEM.NKR. *Retrovirology* **6,** 31 (2009).

53. Vetter, M. L. & D'Aquila, R. T. Cytoplasmic APOBEC3G Restricts Incoming Vif-Positive Human Immunodeficiency Virus Type 1 and Increases Two-Long Terminal Repeat Circle Formation in Activated T-Helper-Subtype Cells. *J. Virol.* **83,** 8646–8654 (2009).

54. Klase, Z. *et al.* Activation of HIV-1 from Latent Infection via Synergy of RUNX1 Inhibitor Ro5-3335 and SAHA. *PLoS Pathog* **10,** e1003997 (2014).

55. Collins, A., Littman, D. R. & Taniuchi, I. RUNX proteins in transcription factor networks that regulate T-cell lineage choice. *Nat. Rev. Immunol.* **9,** 106–115 (2009).

56. Miyoshi, H. *et al.* t(8;21) breakpoints on chromosome 21 in acute myeloid leukemia are clustered within a limited region of a single gene, AML1. *Proc. Natl. Acad. Sci.* **88,** 10431–10434 (1991).

57. Deeks, S. G. HIV: Shock and kill. *Nature* **487,** 439–440 (2012).

BIOGRAPHY

Taylor Goad graduated from Clarke County High School, Berryville, Virginia, in 2008. He received his Bachelor of Science in Biology from George Mason University in 2012.